Romanian Journal of Civil Engineering, Volume 17 (2026), Number 3

Elastoplastic Modelling of the Axial Soil–Pile Interaction

Modelarea elastoplastică a interacțiunii axiale sol–pilot

Mohamed Lamara[1], Ahmed Merah[2], Tayeb Bouziani[3], Houssam Khelalfa[1,4]

[1] LGCE, University of Jijel, Jijel, Algeria
E-mail: *khelalfahoussam@gmail.com*

[2] Faculty of Civil Engineering and Architecture, Research Laboratory of Civil Engineering (LRGC), University Ammar Telidji of Laghouat, Laghouat, Algeria
E-mail: *a.merrah@lagh-univ.dz*

[3] Structures Rehabilitation and Materials Laboratory (SREML), Department of Civil Engineering, University Amar Telidji of Laghouat, Algeria
E-mail: *t.bouziani@lagh-univ.dz*

[4] Faculty of Engineering and Technology, Selinus University of Science and Literature (SUSL), Ragusa, Italy
E-mail: *khelalfahoussam@gmail.com*

DOI: 10.37789/rjce.2026.17.3.2

Abstract
The development of numerical analysis and the significant progress made in the field of computing have made it possible to consider the increasingly complex behaviour of geo-materials. Using the finite element method and an elastoplastic approach, a model of the behaviour of an axially loaded soil–pile system is proposed. The effect of soil–structure interaction is incorporated through interface elements. The soil is represented by a Mohr-Coulomb model with perfect plasticity. For the numerical analysis of soil–pile behaviour, a nonlinear finite element computation code has been developed. Ultimate loads are determined for a pile subjected to axial compression and tension. The results obtained highlight the importance of the contact zone on the distribution of stresses within the soil.

Keywords: *Geo-materials, soil–structure interaction, elastoplastic behaviour, piles, interface elements, ultimate loads.*

1- INTRODUCTION

The behaviour of geo-materials is often modelled within the framework of linear elasticity. However, experimental results have shown that stress–strain relationships are nonlinear and that part of the deformations is irreversible. It is therefore more appropriate to consider the nonlinear (elastoplastic) nature of these materials when

The article was received on 24.06.2026, accepted on 11.09.2026 and published on 22.09.2026

modelling their behaviour. The advancement of numerical calculation models has made it possible to account for the increasingly complex behaviour of geo-materials. In this field of research, the finite element method (Zienkiewicz, 1973) can be considered an effective and practical tool for simulating the behaviour of foundation soils. One of the main advantages of this method is its ability to handle various issues such as variations in soil properties, complex boundary conditions, and different loading cases.

The modelling of contact problems is a matter of great importance in soil and rock mechanics, whether dealing with contact between two different soil layers, fractures in rock masses, or soil–structure interaction. In such cases, it is not acceptable to neglect the effect of relative movements at the contact zones on the overall behaviour of the structure. For a more accurate numerical analysis of these problems, interface elements have been proposed by various researchers to model soil–structure interaction while considering the relative displacements at the interfaces.

The prediction of the nonlinear response of deep foundations under vertical loads is an important problem in soil–structure interaction. A realistic approach to the analysis of deep foundations must take into account the post-elastic behaviour of the soil. The main objective of this work is to model, using the finite element method, deep foundations subjected to axial loading. The behaviour of the soil–pile system is governed by a Mohr-Coulomb type law. The contact zones are represented by thin layer interface elements. The nonlinear system of equations is solved using an incremental-iterative method with a tangent stiffness matrix to improve convergence. Based on the formulation of the various elements (finite elements and interface elements), a computational code named ANAPLAST, written in Fortran, has been developed in this study.

2- ELASTOPLASTIC BEHAVIOUR OF GEO-MATERIALS.

A material is said to exhibit elastoplastic behavior when, beyond a certain loading level (the yield threshold), it undergoes irreversible (plastic) deformations in addition to reversible (elastic) deformations. More generally, and for three-dimensional cases, the yield threshold is replaced by a surface in stress space, described by a function known as the yield function or plasticity criterion, such that:

$$\text{if} \quad \begin{cases} F(\sigma) < 0, & \text{the material behaviour is within the elastic domain.} \\ F(\sigma) > 0, & \text{the material behaviour is within the plastic domain.} \end{cases}$$

2-1- Steps for Formulating an Elasto-plastic Constitutive Law

The formulation of an elastoplastic constitutive law is based on plasticity theory, incorporating an associated flow rule and isotropic hardening. The total strain rate $\mathbf{d\varepsilon}$ is decomposed into an elastic part and a plastic part:

$$\mathbf{d\varepsilon} = \mathbf{d\varepsilon^e} + \mathbf{d\varepsilon^p}$$

Where $\mathbf{d\varepsilon}$, $\mathbf{d\varepsilon^e}$ and $\mathbf{d\varepsilon^p}$ are the total, elastic, and plastic strain rates, respectively.

Plastic deformation occurs when the stress state reaches the yield surface $\mathbf{F}(\sigma) = 0$. The direction of this plastic strain increment is defined by the plastic potential function $\mathbf{g}(\sigma)$. The normal to this surface is determined by the flow rule.

$$\left(\mathbf{d\varepsilon_{ij}}\right)_{\mathbf{p}} = \mathbf{d\lambda} . \frac{\partial \mathbf{g}}{\partial \sigma_{\mathbf{ij}}}$$

Where $\mathbf{d\lambda}$ is the proportionality constant known as the plastic multiplier, this equation is referred to as the flow rule. When $\mathbf{g}$ is different than $\mathbf{F}$ the material is said to follow a non-associated plasticity model, distinguishing between a yield function and a plastic potential function. However, the relation $\mathbf{F} \equiv \mathbf{g}$ holds a particular significance in plasticity theory; in this case, it is known as associated plasticity, and the material is considered "standard Applying the consistency condition.

$$\mathbf{dF} = \left\{\frac{\partial \mathbf{F}}{\partial \boldsymbol{\sigma}}\right\} . \mathbf{d}\boldsymbol{\sigma} + \left\{\frac{\partial \mathbf{F}}{\partial \boldsymbol{\kappa}}\right\} . \mathbf{d}\boldsymbol{\kappa} = \mathbf{0}$$

Where $\mathrm{d}\kappa$: the hardening parameter

After developing and arranging the various terms, the elastoplastic relationship between stress increments and strain increments is obtained as:

$$\mathbf{d}\boldsymbol{\sigma} = \left[\mathbf{D^e} - \frac{\mathbf{D^e} . \left\{\frac{\partial \mathbf{g}}{\partial \boldsymbol{\sigma}}\right\} \left\{\frac{\partial \mathbf{F}}{\partial \boldsymbol{\sigma}}\right\} \mathbf{D^e}}{-\left\{\frac{\partial \mathbf{F}}{\partial \boldsymbol{\kappa}}\right\} . \left\{\frac{\partial \mathbf{g}}{\partial \boldsymbol{\sigma}}\right\} + \left\{\frac{\partial \mathbf{F}}{\partial \boldsymbol{\sigma}}\right\} . \mathbf{D^e} . \left\{\frac{\partial \mathbf{g}}{\partial \boldsymbol{\sigma}}\right\}} \right] . \mathbf{d}\boldsymbol{\varepsilon} \quad \text{Or simply} \qquad \mathbf{d\sigma} = \mathbf{D^{ep} d\varepsilon}$$

$\mathbf{D^e}$: is the elastoplastic constitutive matrix

This relationship between stress increments $\mathbf{d\sigma}$ and strain increments $\mathbf{d\varepsilon}$, defines the transition from the elastic state to the elastoplastic state, which is characterized by a reduction in stiffness once the stress threshold is exceeded.

2-2- Failure Criterion

A failure criterion is represented by a yield function, which may incorporate strain hardening. In this study, a Mohr-Coulomb type criterion is adopted. This criterion states that failure occurs according to the following relation: $|\tau| = \mathbf{f}(\sigma)$. This relation can be expressed in the form of:

$$\mathbf{F}(\sigma) = (\sigma_1 - \sigma_3) - (\sigma_1 + \sigma_3) . \mathbf{sin}(\varphi) - 2 . \mathbf{c} . \mathbf{cos}(\varphi) = 0$$

This corresponds to the equation of a plane, whose intersection with the hydrostatic axis ($\sigma_1 = \sigma_2 = \sigma_3$) occurs at the point defined by $H = -c.\cot g\varphi$. Where $\sigma_1 > \sigma_2 > \sigma_3$, c:is the cohesion et φ: is the internal friction angle. The generalization of the Mohr-Coulomb criterion in the three-dimensional stress space results in the equation of a pyramid with a non-uniform hexagonal base (the failure surface), whose axis is aligned with the hydrostatic axis. The Mohr-Coulomb criterion is often employed in soil behaviour modelling due to its simplicity and because its parameters have clear physical meaning. However, this criterion has certain limitations, such as singularities at the corners of the pyramid (i.e. discontinuities in the yield surface at specific stress combinations).

2-3- Alternative Form for Numerical Calculation

To facilitate numerical implementation, it is particularly convenient to rewrite the yield function in terms of the stress invariants. The main advantage of this formulation is that it allows coding the yield function and the flow rule in a more general form, requiring only the specification of three constants for each failure criterion. The principal stresses σ_1 ,σ_2 ,σ_3 are expressed in terms of the stress invariants as follows:

$$\begin{Bmatrix}\sigma_1\\ \sigma_2\\ \sigma_3\end{Bmatrix} = \frac{2(J_2)^{\frac{1}{2}}}{\sqrt{3}}\begin{Bmatrix}\sin\left(\theta+\frac{2\pi}{3}\right)\\ \sin\theta\\ \sin\left(\theta+\frac{4\pi}{3}\right)\end{Bmatrix} + \frac{I_1}{3}\begin{Bmatrix}1\\1\\1\end{Bmatrix} \quad \text{Where } \sigma_1 > \sigma_2 > \sigma_3 \quad \text{et} \quad -\pi/6 < \theta < \pi/6.$$

I_1 : the first invariant of the total stress tensor, J_2: the second invariant of the deviatoric stress tensor, θ : a parameter defined by the Lode angle $\sin(3\theta) = -3\sqrt{3}J_3/2(J_2)^{3/2}$, which replaces J_3 the third invariant of the deviatoric stress tensor.

The Mohr-Coulomb failure criterion can thus be reformulated in terms of $\mathbf{I_1}$, $\mathbf{J_2}$ et θ. After substituting the principal stresses, the expression becomes:

$$F(I_1,J_2,\theta) = \frac{1}{3}I_1\sin\varphi + (J_2)^{\frac{1}{2}}\left(\cos\theta - \frac{1}{\sqrt{3}}\sin\theta\cos\varphi\right) - c\cos\varphi = 0$$

In order to evaluate the elastoplastic constitutive matrix $\mathbf{D^{ep}}$, it is necessary to express the flow vector $\{\mathbf{a}\}^{\mathbf{T}}$ in a form more suitable for numerical computation.

$$\{a\}^{T} = \frac{\partial F}{\partial\sigma} = \frac{\partial F}{\partial I_1}\frac{\partial I_1}{\partial\sigma} + \frac{\partial F}{\partial (J_2)^{\frac{1}{2}}}\frac{\partial (J_2)^{\frac{1}{2}}}{\partial\sigma} + \frac{\partial F}{\partial\theta}\frac{\partial\theta}{\partial\sigma} \quad \text{Where} \quad \{\sigma\}^{T} = \{\sigma_x,\sigma_y,\sigma_z,\tau_{xy},\tau_{yz},\tau_{zx}\}.$$

This formulation allows for a more flexible and efficient implementation of the yield criterion and the flow rule within a finite element analysis code.

3- INTERFACE ELEMENT CONCEPT

Interface elements were first introduced by Goodman et al. (1968) for the numerical analysis of rock masses. They were soon extended to the study of soil-structure interaction by several researchers such as Zienkiewicz et al. (1991), Ghaboussi et al. (1973), Desai et al. (1984), among others. In a two-dimensional case, the stress-displacement relationship for an interface element is expressed as:

$$\begin{Bmatrix} \sigma_n \\ \tau \end{Bmatrix} = \begin{pmatrix} K_n & 0 \\ 0 & K_s \end{pmatrix} \begin{Bmatrix} V_r \\ U_r \end{Bmatrix} = [C] \begin{Bmatrix} V_r \\ U_r \end{Bmatrix}$$

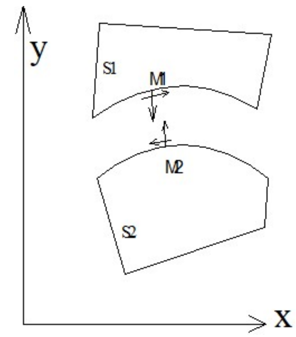

Where σ_n, τ : are the normal and shear stresses;

K_n, K_s : are the normal and tangential stiffnesses;

V_r, U_r : are the relative normal and tangential displacements.

In this study, a thin-layer type interface element was adopted, based on the formulation by Desai et al. (1984). This is an eight-node element with a given thickness t. The major advantage of this element type is that it can be integrated into a finite element code without requiring additional special functions, such as Lagrange multipliers or penalty functions. It is treated like any other solid finite element, with the difference being in the constitutive matrix formulation. The constitutive matrix for this element is:

$$[C]_i = \begin{bmatrix} C_{nn} & C_{nt} \\ C_{tn} & C_{tt} \end{bmatrix}$$

Where : C_{nn} ; C_{tt} : are the normal and tangential stiffness components

C_{tn} : The matrix includes coupling effects between normal and tangential behaviors if required.

The element stiffness matrix for the interface element is then assembled as:

$$[K]_i = \int_v [B]^t \left[C^{ep}\right][B]\,dv$$

$[B]$: is the strain-displacement matrix; $\left[C^{ep}\right]$: is the elastoplastic constitutive matrix specific to the interface behaviour.

The integration is performed over the element's volume, this allows for a realistic simulation of the contact behaviour between materials with very different mechanical properties (such as concrete and soil) under various loading conditions.

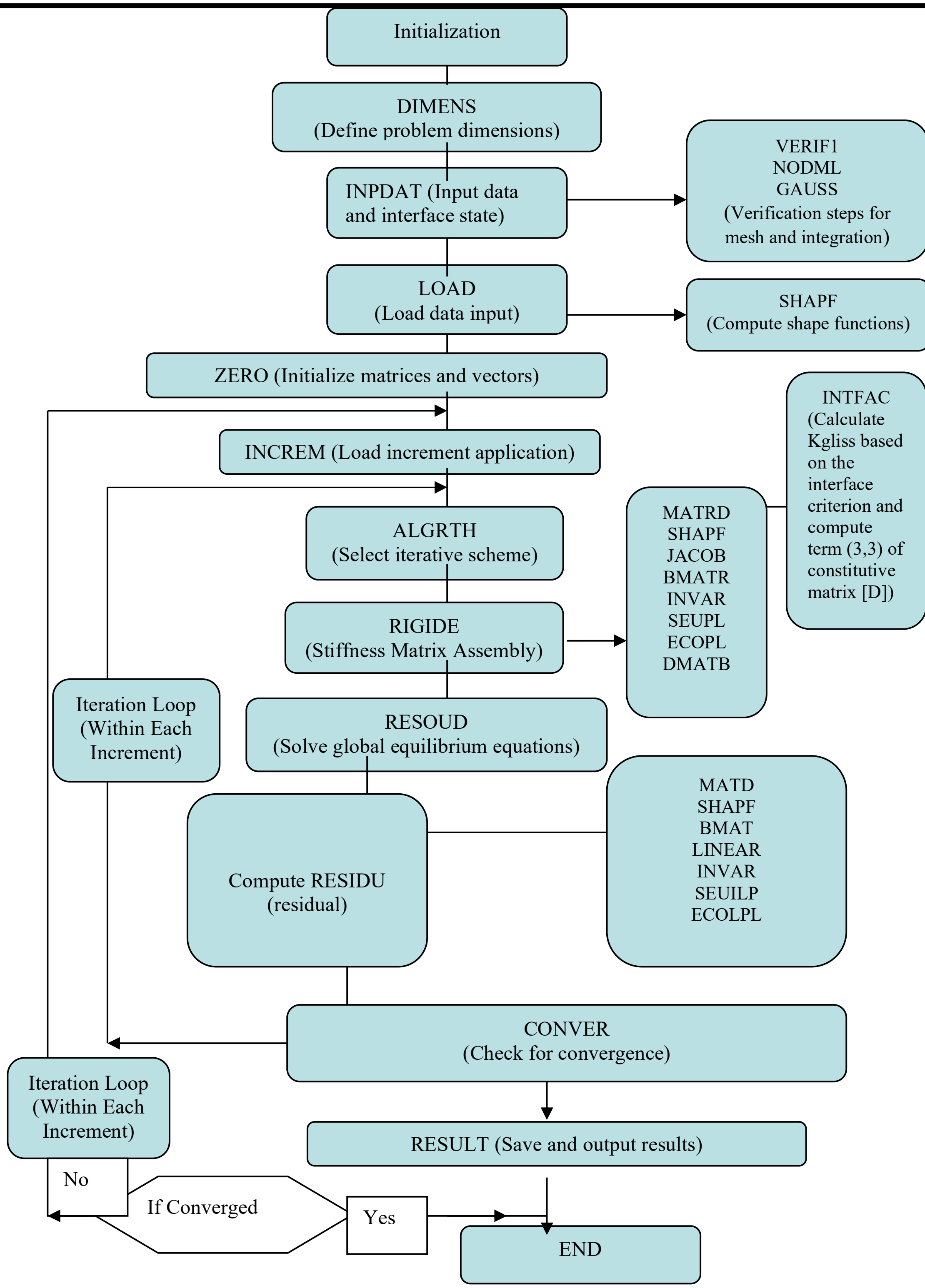

Figure (1) : General Flowchart of the Elasto-Plastic Program ***ANAPLAST***

4- APPLICATION

Drawing inspiration from full-scale experimental results of a single bored pile installed through a multilayered soil profile, conducted by the School of Engineering of São Carlos, University of São Paulo in Brazil (Marilza et al., 2001), as well as numerical results obtained by LCPC (using the CESAR code), a numerical modeling of soil–pile behavior was performed using the ANAPLAST code. Two cases were considered: simulation with and without interface elements under axial loading in both tension and compression.

Since the pile studied is cylindrical with a circular cross-section and is axially loaded, the modeling can be carried out under axisymmetric conditions. In our case, the four soil layers and the pile were modeled using eight-node quadratic elements. The dimensions of the mesh domain were chosen such that the lateral boundary is located at a distance of $60\,r_0$ (where r_0 is the pile radius). The lower boundary is positioned at a depth of 1.94 l below the pile tip (where l is the pile length).

- **Present study**: Number of nodes: 198 and number of elements: 55
- **LCPC study**: Number of nodes: 242 and number of elements: 70

The constitutive behaviour adopted for the different soil layers is an associated elastoplastic model, with a Mohr-Coulomb failure criterion. An implicit scheme is used to integrate the constitutive law. The model parameters for each soil layer used in this study are summarized in Table (1).

Tableau (1): *Table 1: Model parameters for the different soil layers.*

Parameters	Depth of sampling (m)			
	1^{er} Layer (0 à 6.3)	2^{eme} Layer (6.3 à 8.3)	3^{eme} Layer (8.3 à 11)	4^{eme} Layer (11 à 20.6)
$E(kPa)$	9150	13510	13570	19300
ν	0.12	0.12	0.07	0.05
$C(kPa)$	13	12	14	17
$\varphi(\deg rés)$	26	23	23	23

The boundary conditions are defined as follows: zero horizontal displacements on the lateral boundary and along the axis of symmetry, and zero vertical displacements at the base.

The behaviour of the pile was modelled under the same experimental conditions used in the full-scale tests, for both types of axial loading: compression and tension. The characteristics of the pile are: diameter 0.35 m, length 7 m, Young's modulus E = $17.3\text{x}10^3$ MPa (in Tension), et E = $29.9\ 10^3$ MPa (in Compression) and Poisson's ratio $\nu = 0.3$. The axial load is applied through variable increments.

a) **Study of Pile Behavior in Compression**

Figures 2-a and 2-b illustrate the variation of the compressive force at the pile head as a function of vertical displacement, for both cases with and without interface elements.

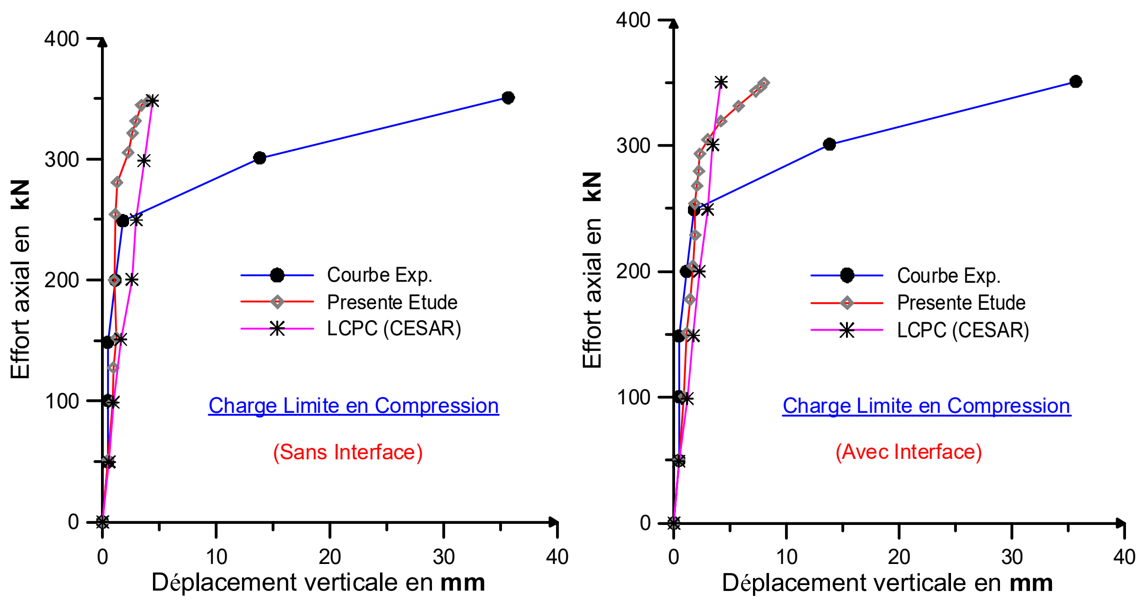

Figure (2) : Axial compressive force versus vertical displacement at the pile head.

The examination of the load–displacement curves shows that, in the linear portion, both numerical analyses exhibit good agreement with the experimental results. The ultimate pile load, approximately P_{lim} = 350 KN, is correctly predicted. However, this load is reached at significantly lower displacements compared to the experimental results. In this study, the modelling incorporating interface elements produces a curve with a characteristic elastoplastic response in the post-elastic region.

Figures 3-a and 3-b show the contours of axial compressive stresses (for cases without and with interface elements, respectively)

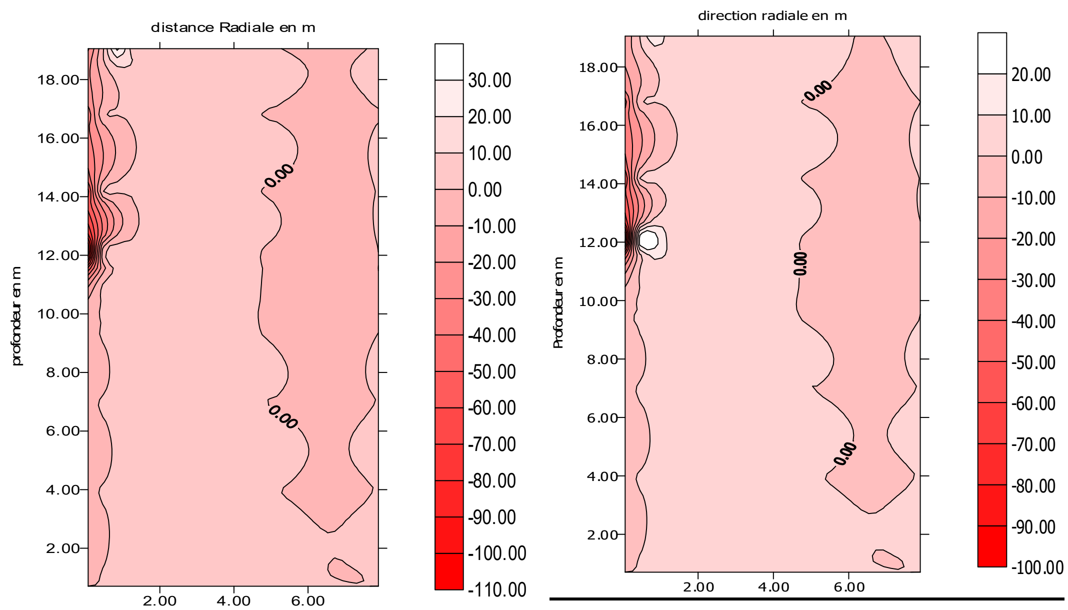

a) Without interface *b) With interface*

Figure (3) : Contour plots of axial stresses σ_{zz} *à 99% at 99% of the total compressive load.*

From these figures, it can be observed that plastic yielding initiates at the pile tip in both cases (with and without interface elements) and progressively spreads upward along the pile shaft. Furthermore, the plastic zones obtained at the end of the calculation remain relatively limited in extent, concentrated near the pile shaft, while a large portion of the surrounding soil mass remains within the elastic domain. It can also be noted that the effect of the interface elements on the distribution of vertical stresses is relatively less significant.

b) **<u>Study of Pile Behaviour in Tension</u>**

Figures 4-a and 4-b present the variation of the axial force at the pile head as a function of its vertical displacement, for the two cases: with and without interface elements. From these figures, it is evident that our program accurately simulates the soil behaviour, even in the vicinity of failure — which is not the case in the study published by LCPC, where the behaviour remains linear up to failure. The analysis shows that the load–displacement curves from our study, especially with interface elements, exhibit a shape similar to that observed in the full-scale test. However, the ultimate load is somewhat underestimated (P_{lim} = 300 kN), which we believe is due to the significant effect of friction under tensile loading.

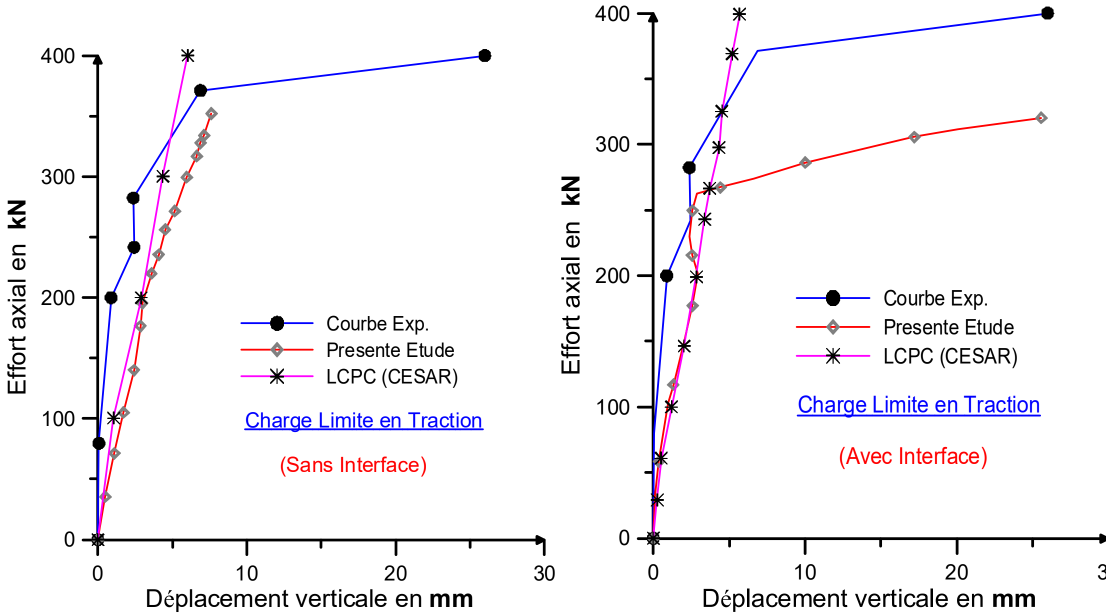

(a) *(b)*

Figure (4) : Axial tensile force versus vertical displacement at the pile head.

Figures 5-a and 5-b display the contours of axial stresses for the tensile case (with and without interface elements, respectively).

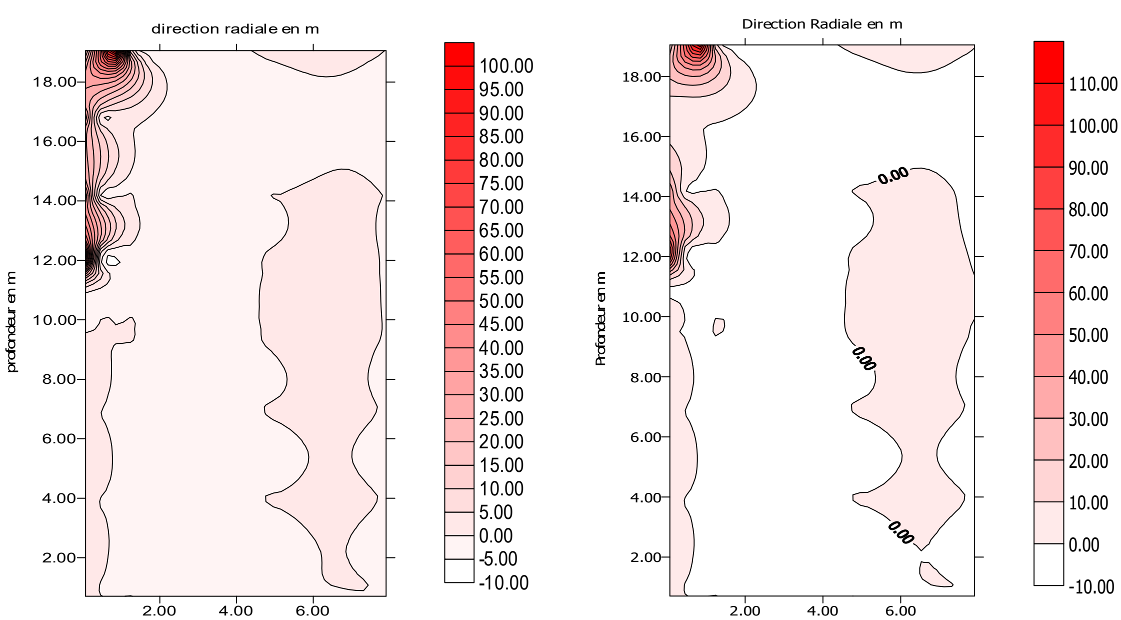

a) *Without interface* b) *With interfacee*

Figure (5) : Contour plots of axial stress σ_{zz} *at 99% of the total tensile load.*

The plastic zones develop initially at the pile tip and then spread toward the ground surface. Moreover, it is observed that the affected zone extends along the entire pile shaft in the case of a perfect bond (without interface elements), while in the case with interface elements, this plastic zone is mainly localized at the pile head and tip. This behavior is likely due to the fact that relative slip between the soil and the pile is prevented in the perfect bond case, thereby mobilizing a larger amount of shaft friction along the pile.

5- CONCLUSION

Through this study, a modelling of the elastoplastic behaviour of geo-materials was presented, taking into account the contact conditions between two materials with significantly different stiffnesses (concrete–soil). The following conclusions can be drawn:

- The initial slope of the load–displacement curve depends primarily on the elastic properties of the soil.
- The ultimate load obtained using our computational program is comparable to that provided by experimental results for the various cases considered.
- The stiffness of the interface does not significantly affect the overall behaviour of the soil; however, it influences the transfer of forces between the two media and the stress distribution within the contact zone.

Finally, the numerical modelling of the elastoplastic behaviour of geo-materials is highly delicate, and achieving convergence in the iterative process is difficult. It depends on both the increment size and the degree of nonlinearity in the constitutive relations. It is recommended for future research to adopt automatic sub-stepping iterative schemes to improve stability and convergence.

REFERENCES

DRUCKER "Soil mechanics and Work hardening theories of plasticity" ASCE, Vol, 122, 1957, pp. 338-346.

DESAI C. S., ZAMAN M.M., LIGHTNER J.G. et SIRIWARDANE "Thin-layer element for interface and joints". Int .Jour for Numerical and analytical Method in Geom. Vol. 8 , 1984 , pp 19-43.

GENS, A., CAROL I. et ALONSO E. E. " An interface of soil reinforcement interaction" Computers and Geotechnics, 1988, pp133-151.

GHABOUSSI J., WILSON E.L et ISENBERG J. "finite element for rock joints and interfaces" –journ of soil Mech and Found Division, Vol, 99 , N° SM10, October 1973, pp 833-848.

GOODMAN R. E., TAYLOR R.L et BREKKE T.L "A model for rock joints and interfaces" journal of the soil Mechanics and foundations Division, Vol , 94 N° SM3, May 1968, pp.637-659.

MARILZA D. N., MESTAT P., FRANK R., DEGNY E. "Etude du comportement des pieux forés" Bulletin LCPC N° 231 /Mars-Avril 2001- pp 55-67.

OWEN DRJ. et HINTON.E "finite element in plasticity theory and practices" Pincridja Press, Swensea, 1980.

SALENCON J. "théorie de la plasticité pour les applications à la mécanique des sols" Éditions Eyrolles.

ZEINKIEWICZ O.C. "la méthode des éléments finis appliquée à l'art de l'ingénieur", 1973 Ediscience Paris.

ZIENKIEWICZ O. C et TAYLOR R.I "The finite element method", Volume 2, 4eme Edition, MC.Graw-Hill, London, 1991.